IOPscience iopscience.iop.org

Home Search Collections Journals About Contact us My IOPscience

The structure of the CoS_2 (100)-(1 × 1) surface

This article has been downloaded from IOPscience. Please scroll down to see the full text article.

2007 J. Phys.: Condens. Matter 19 156223

(http://iopscience.iop.org/0953-8984/19/15/156223)

View the table of contents for this issue, or go to the journal homepage for more

Download details:
IP Address: 129.252.86.83
The article was downloaded on 28/05/2010 at 17:40

Please note that terms and conditions apply.

IOP PUBLISHING JOURNAL OF PHYSICS: CONDENSED MATTER

J. Phys.: Condens. Matter **19** (2007) 156223 (9pp) doi:10.1088/0953-8984/19/15/156223

The structure of the CoS_2 (100)-(1 × 1) surface

Z X Yu[1,2], M A Van Hove[2], S Y Tong[2], David Wisbey[3], Ya B Losovyj[3,4], Ning Wu[5], M Manno[5], L Wang[5], C Leighton[5], W N Mei[3,6] and P A Dowben[3,7]

[1] School of Physics and Engineering, Zhongshan University, Guangzhou 510275, People's Republic of China
[2] Department of Physics and Materials Science, City University of Hong Kong, Kowloon, Hong Kong SAR
[3] Department of Physics and Astronomy and the Nebraska Center for Materials and Nanoscience, University of Nebraska-Lincoln, Lincoln, NE 68588-0111, USA
[4] Center for Advanced Microstructures and Devices, Louisiana State University, 6980 Jefferson Highway, Baton Rouge, LA 70806, USA
[5] Department of Chemical Engineering and Materials Science, University of Minnesota, Minneapolis, MN 55455, USA
[6] Department of Physics, University of Nebraska at Omaha, Omaha, NE 68182-0266, USA

E-mail: pdowben@unl.edu

Received 8 January 2007, in final form 23 January 2007
Published 26 March 2007
Online at stacks.iop.org/JPhysCM/19/156223

Abstract
Quantitative low-energy electron diffraction (LEED) has been used to determine the structure of the cubic CoS_2 (100)-(1 × 1) surface. The clearly favoured structural model from the LEED analysis is the 1S-terminated (1 × 1) surface, in which the S–S dimer is intact and the terminal surface layer retains a complete S–Co–S sandwich structure. The surface S atoms move outwards towards the vacuum while the subsurface Co atoms move towards the bulk, by approximately 0.03 and 0.11 Å, respectively. In addition, the S atoms in the third sublayer relax outwards by about 0.12 Å, thus providing an indication of a stronger S–S dimer bond and a denser surface region. The complete atomic coordinates of the S–Co–S surface layers are determined in this analysis.

1. Introduction

Although undoped CoS_2 is far from an ideal half-metallic ferromagnet, with an electron spin polarization of about 56% as determined from point-contact Andréev reflection [1], CoS_2 remains highly spin polarized with a Curie temperature in the range of 116–120 K [2]. While the pyrite-type transition metal compound CoS_2 is known to be an itinerant electron ferromagnet, few studies have addressed the surface structure. An accurate determination of

[7] Author to whom any correspondence should be addressed.

the surface structure is essential for understanding electron spectroscopy studies, as well as providing a starting point for modelling the interface properties, essential for modelling any spintronics device applications [3]. Photoemission is very surface sensitive, although few of the prior photoemission studies detail any effort at characterization of the surface structure or surface stoichiometry [4–7]. The determination of the surface is important as the free enthalpy of the surface is generally very different from the bulk, so a simple truncation of the bulk structure is not generally the stable surface, as this is not a minimum energy surface. For most high polarization materials, the consequences of a high surface energy (even for a low index surface) are the existence of surface states, surface reconstructions or surface segregation [8].

LEED intensity versus voltage data, when complemented by dynamical scattering calculations, i.e. $I(V)$ analysis, are a useful complement to photoemission band structure, since this provides an independent confirmation of the inner potential, as has been determined from the critical points of the bulk band structure in a companion paper [7].

2. Experiment

The success of this work was made possible by the cleavage of sufficiently large CoS_2 (100) single crystals (millimetres in diameter). The crystals were prepared by chemical vapour transport, and have a well-controlled stoichiometry as detailed in a previous publication [2]. These crystals, when cleaved, provide low energy electron diffraction (LEED) patterns characteristic of a highly ordered surface, as seen in figure 1. We have observed that when cleaving crystals in ambient air, LEED images are also possible following insertion of the sample into ultrahigh vacuum, while low energy electron beam irradiation improves the surface quality and reduces surface contamination of such surfaces.

The LEED experiments were taken in the same ultrahigh vacuum (UHV) chamber as the photoemission data, with a pressure of 1×10^{-10} Torr. Surface composition and order are seen to be strongly dependent upon surface preparation, but the samples appear to be single crystals with no evidence of twinning or grain boundaries in the LEED or x-ray diffraction. The results presented here are restricted to stoichiometric surfaces, prepared by cleaving the crystals to prepare a new surface, and characterized by wave vector dependent photoemission studies [3]. Several sets of data were taken, for several sets of samples. The LEED intensities were obtained as a function of kinetic energy, using a CCD camera.

3. Computational methods

The multiple scattering LEED analysis was performed using an automated tensor LEED program [9, 10], which is capable of very efficient surface-structure determinations. Ordinarily, to proceed with a complex surface structure search we need a computation effort that scales with N^3, where N is the number of atoms in the surface unit cell. Thus it is desirable to use a scheme that will expedite the search and quickly explore a large volume of parameter space. Tensor LEED provides this approach. A full dynamical calculation is first performed for a guessed reference structure. The scattering amplitudes due to small movements of each atom on the surface are then calculated by using the first-order perturbation theory, as a linear function of the individual atomic scattering amplitudes. The method includes corrections from scattering by atoms surrounding the one displaced. Naturally, the utility of this approach depends on how far atoms can be displaced while maintaining the validity of first-order perturbation theory upon which tensor LEED analysis is based. Afterwards, a steepest-descent searching algorithm is employed to seek the best structure amongst the potential models. During the search, approximated theoretical intensities are computed for different trial structures distorted

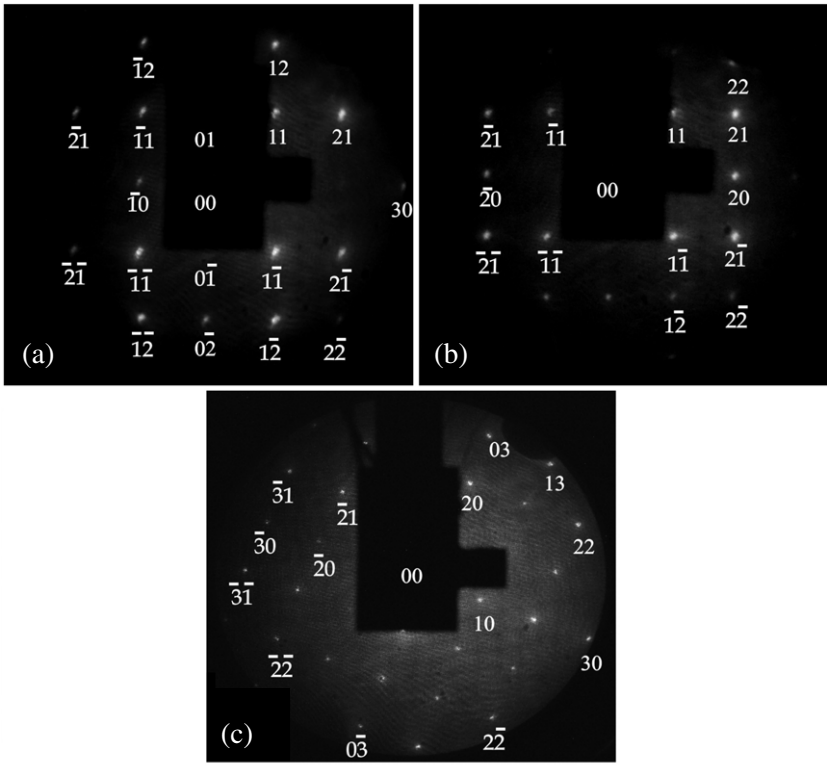

Figure 1. A LEED images of the CoS_2 (100) surface, with various diffraction beams indexed. The kinetic energies are 95 eV (a), 111 eV (b) and 135 eV (c). One LEED image is tilted, so that some of the beams obscured by the sample holder can be observed.

from the reference structure in an efficient manner. Calculated intensities are then used for comparison with the experimental data. Agreement between theory and experiment was assessed using the Pendry reliability factor (R_P).

From the LEED pattern analysis, described later (*vide infra*), it was clear that we must address the glide symmetry present in this system. In the tensor LEED program, the glide symmetry is not fully considered. We cannot increase the speed of the calculations by inclusion of such symmetry considerations nor can we maintain the symmetry in the optimization of structure. Nonetheless, the correct symmetry must be retained when searching for the best-fit structural models. Any other course could lead to an incorrect model and/or large errors. To resolve this problem, we employ a hybrid approach. We first perform a full dynamic calculation for the (starting) reference structure without glide symmetry. In this step, necessary tensors are produced for each atom in the surface region. Then, in the second (optimization) step, we use the glide symmetry to restrict the adjustment of structural parameters. During optimization, only parameters of independent atoms are changed, and thus the positions of each atom in the surface are determined by glide symmetry. Then the theoretical intensities can be quickly computed for any trial structures, making use of the tensors already generated for each atom in the first step.

The input parameters of the fully dynamical calculation are primarily composed of the scattering phase shifts of the Co and S atoms, which are generated from the Barbieri–Van Hove phase shift package. A total of 10 phase shifts ($l_{max} = 9$) was used in the calculations.

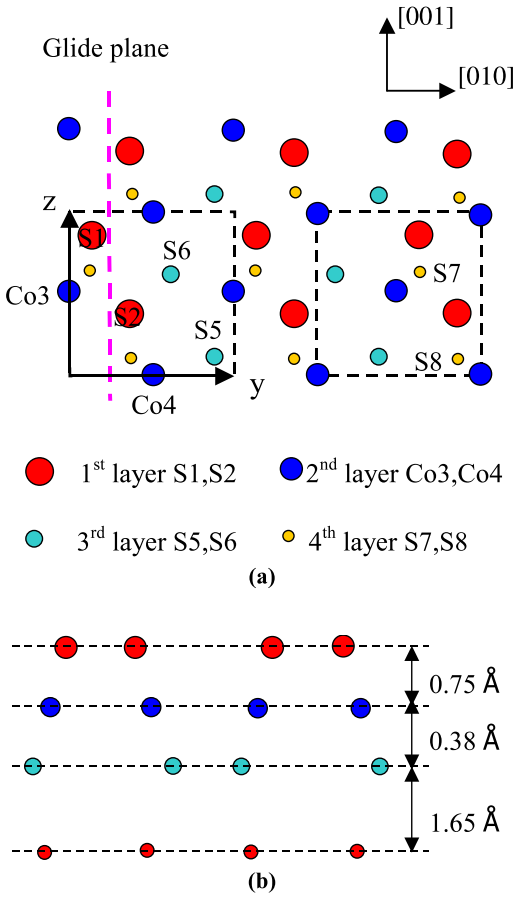

Figure 2. Top (a) and side (b) view of the CoS_2 (100) surface structure and unit cell.

Non-structural parameters include the Debye temperatures and the inner potential. The Debye temperatures for Co and S were first set to 500 K. The energy independent real and imaginary parts of the inner potential (V_r, V_i) were initially set to 5.0 and −4.0 eV, respectively. These non-structural parameters are fixed at the initial stage of the analysis and, together with structural parameters, were optimized in the final refinement of the favoured structures.

4. Surface structure of CoS_2 (100)-(1 × 1)

In figure 2, we show top and side views of the (100) CoS_2 surface and the surface unit cell. Here we have used the convention that the y and z axes are in the 2D surface plane and the x axis points down into the surface (along the surface normal). The bulk CoS_2 has a pyrite-type structure with Co atoms located at the corners and the face centres of a cubic unit cell and eight S atoms located at the positions $\pm(u, u, u)$, $\pm(u + 1/2, 1/2 - u, \bar{u})$, $\pm(\bar{u}, u + 1/2, 1/2 - u)$, $\pm(1/2 - u, \bar{u}, u + 1/2)$, in which u (0.389) is a structural parameter [11, 12], as indicated in figure 3. Since the space group is $T_h^6(Pa3)$, there are no simple symmetries (rotation, mirror or both) in the two-dimensional surface plane. Instead, glide planes normal to the surface are expected. The surface must be a low index face, as it is a cleavage plane, and parallel to the

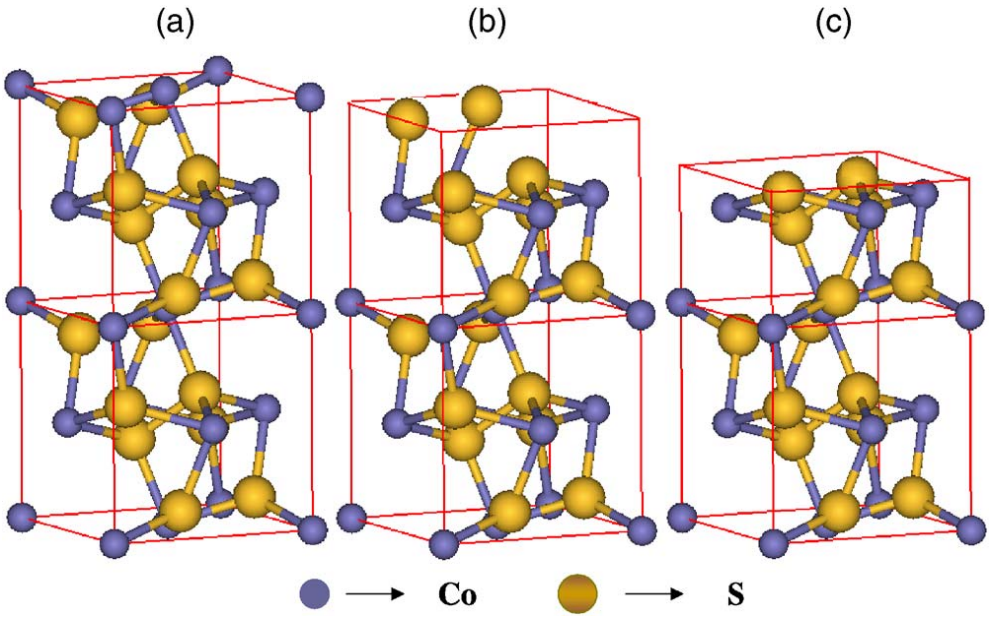

Figure 3. Schematic diagram of possible terminations of the CoS_2 (100) surfaces: (a) Co-terminated, (b) 2S-terminated (by removing a Co layer from the Co-terminated structure) and (c) 1S-terminated (by removing the surface S layer from the 2S-terminated structure).

⟨100⟩ direction determined by XRD. The LEED images (figure 1) establish that this surface is indeed the (100) surface, because of the clear 1×1 structure and four-fold symmetry between spots. In fact, there is no other plane that can be easily cleaved for this material.

For the CoS_2 (100) surface, we chose the bulk-implied square unit cell, with a lattice constant of 5.524 Å. From the numerous LEED patterns we have acquired there are two mirror planes between spots, which are along the [001] and [010] directions, respectively. One mirror plane results from a glide plane along the [001] direction normal to the (100) surface. Usually, missing LEED spots are a signature of a glide plane in the real space structure. In our experiment, the systematically very weak intensities of the LEED spots $(0\bar{1})$ and $(0\bar{3})$ suggest that there is a glide plane along the [001] direction normal to the (100) surface.

As shown in figure 2(a), there exists a glide plane parallel to the z-axis [001]. A glide plane is described by a reflection across a (glide) plane plus a translation parallel to that plane. Crystal periodicity requires that the translation distance is half of the lattice constant in the direction of translation. For example, S1 is related to S2 (as labelled in figure 2) by moving S1 along the glide plane by 2.76 Å (half the lattice constant) and then reflecting across the glide plane. From figure 2(a), we can see there are two possible domains. The first and fourth layers can be grouped into pairs of sublayers, where the two surface terminations have exactly opposite surface geometrical orientations to each other. For example, the atomic positions (S1, S2) in the first sublayer are related to those (S7, S8) of the fourth sublayer by inversion. Of course, there is a three-layer height difference, with half of a lattice constant (2.76 Å), between them. If these layers form terraces on such a surface, they can form domains with mutually opposite surface geometrical orientations. The neighbouring terraces rotate 180° and the final symmetry has two mirror planes. So, the overall symmetric features of the LEED patterns are well explained by the existence of a glide plane, together with a two-domain structure.

Figure 3 illustrates three possible types of surface terminations for the (100) plane of pyrite CoS_2:

(a) Co-terminated (abbreviated as Co-term),
(b) 2S-terminated (abbreviated as 2S-term), by removing the surface Co layer from the Co-term structure, and
(c) 1S-terminated (abbreviated as 1S-term), by removing the surface S layer from the 2S-term structure.

From the structure presented in figures 3(a)–(c), it is clear that there are two domains with a three-layer height difference. So in order to compute the LEED intensities, we have to perform averages over two domains that differ by 180° in rotation. These two domains are assumed to have the same unit cell and structural parameters. In our search for the best surface structure, these two-domain averages were carried out on all the Co-term, 2S-term and 1S-term models. Regarding the experimental side of the data, we have to average all the beams related by two mirror planes. After averaging, six inequivalent experimental beams are used for the structural determination.

In each sublayer there are either two Co atoms or two S atoms. However, only one Co or one S atom is independent because of glide symmetry. As mentioned above, glide symmetry was applied in our optimization, so the number of fitting parameters was reduced by half. Since the distance between Co and S sublayers in the bulk is only about 0.61 Å, this Co–S bilayer cannot be treated as two separate layers in the LEED calculations. Depending on the surface terminations, two to four such bilayers were treated as composite planes, in which only atomic positions that include vertical and lateral parameters of each atom were allowed to vary in the first optimization.

Model (c) (in figure 3) led to the lowest R-factor (R_P, 0.26), and is thus the best-fit structure. The minimum R-factors of the other two terminations were found to be 0.47 and 0.49, respectively. We have therefore ruled out models (a) and (b) as possibilities and regard model (c) (in figure 3) as the most favourable surface termination.

5. Relaxation of the surface structure

At the final stage of refinement, both the structural parameters and the non-structural parameters (i.e. the Debye temperature and the inner potential) are optimized for the favoured S-terminated model (c) (in figure 3). In this model, the first three sublayers of Co and S are allowed to vary to obtain optimization of the surface and subsurface structure, while the deeper layers are treated as bulk. This further optimization step does not lead to a significant improvement on the R-factor, yielding a final structure with an R_P of 0.23. The optimal values for the structural and non-structural parameters are listed in table 1. In general we found that the atoms in S and Co sublayer relax, respectively outward (toward the vacuum) and inward (toward the bulk), along the surface normal ('x'), by approximately 0.03 and 0.11 Å. In addition, the S atoms in the third sublayer move out (toward the vacuum) by about 0.12 Å. As a result of these surface layer relaxations, the width (thickness) of the outermost Co–S bilayer is expanded from 0.61 to 0.75 Å, while that of the subsurface Co–S bilayer contracts significantly from 0.61 to 0.38 Å. The vertical distance between the third sublayer and the bulk is altered from 1.53 to 1.65 Å, as shown in figure 2(b). The relevant bond lengths of the Co–S pairs are calculated to be 2.13 and 2.42 Å, respectively. These values represent a 4 to 8% change in the Co–S bond length, compared to a bulk value of 2.32 Å. The bond distance of the S–S dimer decreases from 2.12 to 2.02 Å, which indicates that much stronger bonds are formed between the S–S dimer pairs. The largest relaxation was found to be less than 0.13 Å for all the structural parameters. In

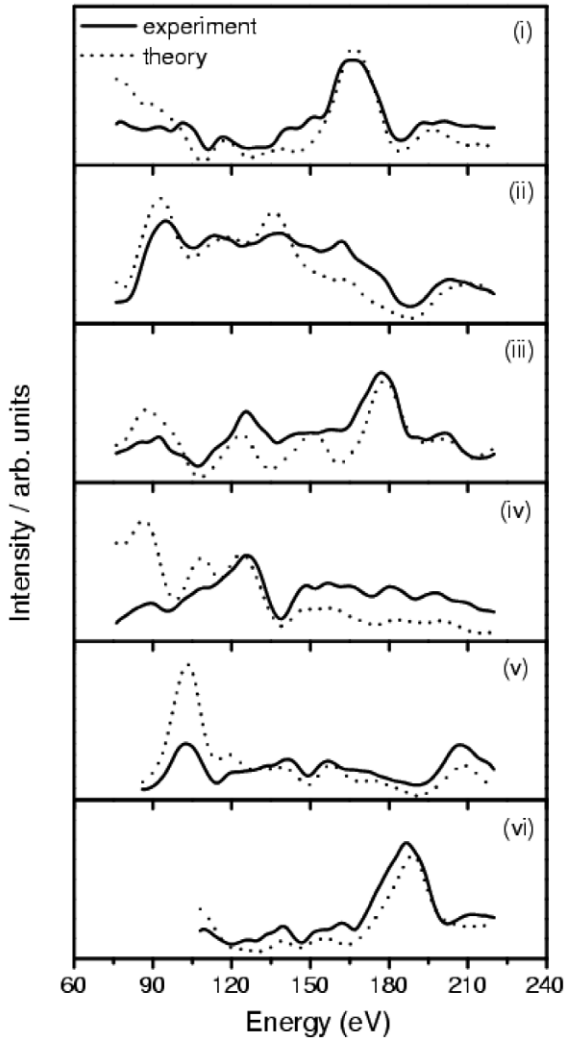

Figure 4. Comparison of measured (solid lines) and calculated (dashed lines) IV spectra for the best-fit structure—a 1S-terminated CoS_2 (100) surface. Here we show the results of the available beams and their R-factors (R_p): (i) $(-1, 0)$, $R_p = 0.30$; (ii) $(1, 1)$ $R_p = 0.15$; (iii) $(2, 0)$, $R_p = 0.28$; (iv) $(2, 1)$, $R_p = 0.29$; (v) $(1, 2)$, $R_p = 0.14$; and (vi) $(3, 0)$, $R_p = 0.23$.

figure 4, we present the LEED experimental spectra for the cubic CoS_2 (100)-(1×1) surface, together with the best-fit calculated spectra. Clearly, there is a rather good agreement between the experimental and theoretical data.

6. Agreement with the bulk band structure

From the critical points of the experimental band structure of CoS_2 [7], we have made an estimate for the inner potential of about 4.8 eV. This is more than a factor of 2 smaller than most transition metals (including Ni [13] and Mo [14]). The LEED analysis produces an independent theoretical quantity of about 3.62 eV, the muffin-tin zero sometimes also called

Table 1. The non-structural and structural parameters of bulk and the best-fit structure—a 1S-terminated CoS_2 (100) surface. Here, y and z are at the surface plane and x is down into the surface. In addition, negative x means moving outward to the vacuum.

	Bulk structure (Å)			Optimized structure (Å)		
Atoms	x	y	z	x	y	z
S1	0.000	0.613	4.911	−0.029	0.697	4.966
S2	0.000	2.149	2.149	−0.029	2.065	2.204
Co_3	0.613	0.000	2.762	0.724	0.120	2.629
Co_4	0.613	2.762	0.000	0.724	2.642	−0.133
S5	1.226	4.911	0.613	1.107	4.942	0.522
S6	1.226	3.375	3.375	1.107	3.344	3.284

$\mathbf{R_p} = \mathbf{0.23}$, $V_r = 3.62$ eV, $V_i = -4.5$ eV, $T_{Co} = 600$ K, $T_S = 800$ K.

the inner potential. This theoretical quantity, from LEED analysis, cannot be measured and thus cannot be directly compared with an experimentally determined inner potential from the photoemission band structure. Although nominally considered a scalar [15], some assessment will need to be made of the electron kinetic energy dependence of the inner potential. In practice, the inner potential can vary somewhat with kinetic energy, typically falling to smaller values at high kinetic energies in both the LEED analysis [16] and photoemission band structure analysis. Still, both the LEED and photoemission values are characteristic of a narrow band system, again consistent with theoretical expectations [7].

7. Conclusions

The surface is characterized by glide plane symmetry, consistent with the pyrite-type structure. Dynamical scattering theory provides good agreement between a relaxed surface structure and experimental LEED $I(V)$ data. Consistent with our newly found ability to cleave CoS_2 (100), the surface of CoS_2 (100) is a densely packed surface, with relatively short Co–S bonds and the sulfur atoms outermost. We find that the surface S and Co atoms relax outward (toward the vacuum) and inward (toward the bulk), along the surface normal, approximately by 0.03 and 0.11 Å, respectively. This results in a larger surface dipole, and a concomitant increase in work function.

Acknowledgments

The authors at the City University of Hong Kong were supported by RGC grant no. 8730017 of Hong Kong. The authors at the University of Nebraska were supported by the Nebraska Research Initiative UNL NSF 'QSPINS' MRSEC (DMR 0213808) and ONR grant no. N00014-06-1-0616. The authors at the University of Minnesota are supported by the UMN NSF MRSEC (DMR-0212302). CAMD is supported by the Louisiana Board of Regents.

References

[1] Wang L, Umemoto K, Wentzcovitch R M, Chen T Y, Chien C L, Checkelsky J G, Eckert J C, Dahlberg E D and Leighton C 2005 *Phys. Rev. Lett.* **94** 056602
[2] Wang L, Chen T Y, Chien C L and Leighton C 2006 *Appl. Phys. Lett.* **88** 232509
[3] Tsymbal E, Belashchenko K, Velev J, Jaswal S, van Schilfgaarde M, Oleynik I and Stewart D 2007 *Prog. Mater. Sci.* **52** 401

[4] Takahashi T, Naitoh Y, Sato T, Kamiyama T, Yamada K, Hiraka H, Endoh Y, Usuda M and Hamada N 2001 *Phys. Rev.* B **63** 094415
[5] Fujimori A, Mamiya K, Mizokawa T, Miyadai T, Sekiguchi T, Takahashi H, Mori N and Suga S 1996 *Phys. Rev.* B **54** 16329
[6] Muro T, Kimura A, Iwasaki T, Ueda S, Imada S, Matsushita T, Sekiyama A, Susaki T, Mamiya K, Harada T, Kanomata T and Suga S 1998 *J. Electron Spectrosc. Relat. Phenom.* **88–91** 361
[7] Wu N, Losovyj Ya B, Wisbey D, Belashchenko K, Manno M, Wang L, Leighton C and Dowben P A 2007 *J. Phys.: Condens. Matter* **19** 156224
[8] Dowben P A and Jenkins S J 2005 The limits to spin-polarization in finite-temperature half-metallic ferromagnets *Frontiers in Magnetic Materials* ed A Narlikar (Berlin: Springer) pp 295–25
[9] Barbieri A and Van Hove M A (http://www.sitp.lbl.gov/index.php?content=/leedpack/)
[10] Rous P J, Pendry J B, Saldin D K, Heinz K, Muller K and Bickel N 1986 *Phys. Rev. Lett.* **57** 2951
[11] Zhao G L, Callaway J and Hayashibara M 1993 *Phys. Rev.* B **48** 15781
[12] Jin Y J and Lee J I 2006 *Phys. Rev.* B **73** 064405
[13] Eberhardt W and Plummer E W 1980 *Phys. Rev.* B **21** 3245
[14] Yakovkin I N, Zhang J and Dowben P A 2001 *Phys. Rev.* B **63** 115408
[15] Ashcroft N W and Mermin N D 1976 *Solid State Physics* (Texas: Saunders)
[16] Clarke L J 1985 *Suface Crystallography: An Introduction to Low Energy Electron Diffraction* (New York: Wiley)